Proceedings Paper:
Duncan, S.R., Fruhnert, M. and Drummond, R. (2025) Control of braking for automatic train operation. In: 2025 IEEE Conference on Control Technology and Applications (CCTA). 2025 IEEE Conference on Control Technology and Applications (CCTA), 25-27 Aug 2025, San Diego, CA, USA. Institute of Electrical and Electronics Engineers (IEEE), pp. 838-843. ISBN: 9798331539092. ISSN: 2768-0762. EISSN: 2768-0770.

https://doi.org/10.1109/ccta53793.2025.11151507

Control of Braking for Automatic Train Operation

Stephen R. Duncan, Michael Fruhnert and Ross Drummond

Abstract— **An important function of an Automatic Train Operation (ATO) system is to control braking to bring a train to a standstill at a specific location in a smooth and safe manner. To minimise journey times and to improve throughput on a rail network, the time required for braking needs to be minimised. This paper considers braking as an optimal, minimum time control problem and applies the solution as a feedforward braking traction. A feedback controller is then used to ensure that the train speed follows the optimal solution. The feedback is based on a PID controller to align with the existing structure of the ATO system. By considering the controller as a Lur'e system, the Popov criterion provides a limit on the allowable slope of the braking curve and the optimal profile is modified to ensure that this constraint is satisfied. The performance of the controller is evaluated on an industry supplied simulation of the train dynamics.**

I. INTRODUCTION

Automatic train operation (ATO) systems often form part of a wider automatic train control (ATC) system, with the ATO focussing on the automatic stopping and starting of the train. This paper considers the problem of bringing a train to a standstill at a specific location, such as a station. During braking, ATO systems typically operate by measuring the position of the train using a series of transponders at discrete locations along the track and adjusting the braking traction so that the train speed follows a braking curve, which relates the speed of the train to its location along the track. To increase the throughput of trains and to reduce journey times, it is desirable to minimise the time for the braking procedure, but it is also necessary to ensure that the train stops at the correct location. This is particularly important when stopping at a station that has screens along the platform, where the doors of the train need to align with doors in the screens on the platform to allow passengers off and on, which requires that the stopping accuracy needs to be within ± 30 cm.

During braking, electric trains typically use a combination of two modes of operation; friction braking, which uses a pneumatic system to apply a brake block to the wheels (this is also referred to as pneumatic or air braking) and electric or regenerative braking, where traction is applied by using motors to generate electricity. Electric braking is more efficient, but has limited effect both at low speeds and at high speeds, so a process of brake blending is used to combine the two modes to achieve the required traction across the full speed range. There is also a mechanical parking brake that is applied once the train has come to a standstill in order to hold the train stationary when stopping on a track with a gradient.

In principle, the braking of the train could be controlled using model predictive control (MPC), which has already been proposed for train operations [1]–[4], but these studies have primarily considered minimising energy usage during train operations. The problem of train braking is also similar to docking ships [5], [6] and landing aircraft [7]. Although computer based systems are increasingly common within trains, often these systems handle a range of other functions and trains do not have the computational capacity to implement MPC, particularly over the relatively long control horizons associated with braking. This paper takes an alternative approach that is closer to the method of operation of existing ATO systems, which makes it more straightforward to implement. A braking curve, which relates the speed of the train to its location along the track, is obtained by solving a minimum time optimisation problem [8] using a simplified model of the train dynamics. Feedback, based on a PID controller, is then used to maintain the train speed on this profile throughout braking, despite the presence of disturbances and model uncertainties. In addition, the traction signal obtained from the solution to the optimisation problem is used as a feedforward signal, so that the PID control only applies relatively small adjustments. By considering the braking curve as a sector bounded, static nonlinearity, the controller can be regarded as a Lur'e system, so that the stability of the system can be checked using the Popov criterion [9]. To maintain stability, the optimal braking curve is modeified to prevent large gains occurring in the feedback loop as the train approaches the stopping point. The performance of the control approach is evaluated on simulations based on the simplified model of train dynamics and on full model that more accurately describes the response of the train during braking.

The paper is organised as follows. Section II introduces the simplified model of the dynamics and uses this as the basis of the minimum time optimisation problem that generates the braking curve and the corresponding feedforward traction signal. Section III designs a PID controller to ensure that the train speed follows the braking curve and determines the modification to the feedforward trajectory that is required to maintain closed loop stability. Simulations based on both the simplified model and a full model of the train dynamics are described in Section IV. Section V concludes the paper.

Stephen R. Duncan is with the Department of Engineering Science, University of Oxford, Oxford OX1 3PJ, United Kingdom. Email: stephen.duncan@eng.ox.ac.uk.

Michael Fruhnert is with Siemens Mobility GmbH., Kiefholzstr. 44, 12435 Berlin, Germany. Email: michael.fruhnert@siemens.com.

Ross Drummond is with the Department of Electrical and Electronic Engineering, University of Sheffield, Sheffield, S1 3JD, United Kingdom. Email: ross.drummond@sheffield.ac.uk.

II. FEEDFORWARD DESIGN

A. System Model

The (normalised) dynamics of the train can be approximated by a first order response of the form

$$\dot{v}(t) = -a^{(i)}v(t) + b^{(i)}u(t-\tau) - g\sin\theta(x(t)), \quad (1)$$

where $v(t)$ is the train speed, $u(t)$ is the applied traction, g is the acceleration due to gravity and $\theta(x(t))$ is the gradient of the track, with $x(t)$ being the distance along the track. There is a time delay τ due to a delay within the control system and a delay associated with applying the traction to the motor. The values of the constants $a^{(i)}$ and $b^{(i)}$ depend on whether the train is driving or braking, as denoted by $i \in \{\mathrm{D}, \mathrm{B}\}$, with $u(t) > 0$ when driving and $u(t) < 0$ when braking. The gradient of the track is assumed to be a piecewise constant function of distance.

Denoting the jerk applied to the train by $j(t)$, the train dynamics can be expressed as

$$\begin{bmatrix} \dot{u}(t) \\ \dot{v}(t) \\ \dot{x}(t) \end{bmatrix} = \begin{bmatrix} 0 & 0 & 0 \\ b^{(i)} & -a^{(i)} & 0 \\ 0 & 0 & 1 \end{bmatrix} \begin{bmatrix} u(t) \\ v(t) \\ x(t) \end{bmatrix} + \begin{bmatrix} j(t-\tau) \\ 0 \\ 0 \end{bmatrix} - \begin{bmatrix} 0 \\ g\,\theta(x(t)) \\ 0 \end{bmatrix}. \quad (2)$$

The nominal values of the parameters $a^{(i)}$ and $b^{(i)}$ and the time delay τ used in this study are given in Table I. Although these parameters are taken to be constants, in practice, there is considerable variation of these values both between different trains and during braking for an individual train, as the braking mode switches between regenerative electrical braking and combined regenerative and pneumatic braking. The model in (1) is a simplified version of the dynamics, so it is also likely that there are additional unmodeled dynamics. The system will also be subject to disturbance, particularly in the applied traction, for example due to wheel slip resulting from wet rails or leaves on the line. For this reason, any control strategy for braking must be designed so that it is robust to model uncertainties, disturbances and variations in the parameters.

a^{D} (s^{-1})	b^{D} ($\mathrm{m.s}^{-2}$)	a^{B} (s^{-1})	b^{B} ($\mathrm{m.s}^{-2}$)	τ (s)
2.2×10^{-3}	1.0	2.6×10^{-4}	1.13	0.3

TABLE I: Values of model parameters used in simulations.

B. Constraints

The traction that is applied to the train during braking is subject to the following constraints.

- The train cannot reverse while braking, so $v(t) \geq 0$.
- During the braking phase, the traction must be negative and it is not permitted to switch between braking and driving, so that $u(t)$ must be negative or zero. In addition, there is a limit on the braking traction $-\underline{u}$ that can be applied to the train, so that

$$-\underline{u} \leq u(t) \leq 0. \quad (3)$$

- To prevent damage to the electric motor and to ensure passenger comfort, there is an input constraint that limits the rate of change of traction

$$-\underline{j} \leq j(t) \leq \bar{j}. \quad (4)$$

The values used for the constraints in this study are given in Table II.

$\underline{u}$ ($\mathrm{m.s}^{-2}$)	$\underline{j}$ ($\mathrm{m.s}^{-3}$)	$\bar{j}$ ($\mathrm{m.s}^{-3}$)
0.96	0.20	0.05

TABLE II: Values of constraints.

C. Optimal Control Problem

To take account of the delay within the system, define $\hat{u}(t) = u(t-\tau)$, so that the response of the train in (1) becomes

$$\dot{v}(t) = -a^{(i)}v(t) + b^{(i)}\hat{u}(t) - g\sin\theta(x(t)), \quad (5)$$

Similarly, defining $\hat{j}(t) = j(u(t-\tau)$, then $\dot{\hat{u}}(t) = \hat{j}(t)$. Once the optimal profile for $\hat{u}(t)$ has been found, the optimal traction can be recovered using $u(t) = \hat{u}(t+\tau)$.

The aim is to bring the train from an initial constant speed v_0 at time t_0, to a standstill at a specific location, x_{f}, in the minimum time. Taking $t_0 = 0$, the initial state of the system is $[\hat{u}_0 \; v_0 \; x_0]^{\mathrm{T}}$. Since the initial train speed is constant, then from (5),

$$\hat{u}_0 = \frac{a^{(\mathrm{D})}v_0 + g\sin\theta(x_0)}{b^{(\mathrm{D})}}. \quad (6)$$

Because the train is brought to a standstill, the final state is $[\hat{u}_{\mathrm{f}} \; 0 \; x_{\mathrm{f}}]^{\mathrm{T}}$ and without loss of generality, it can be assumed that $x_{\mathrm{f}} = 0$, which means that the initial position of the train satisfies $x_0 < 0$. It is assumed that the track has zero gradient at the desired stopping point for the train, so that $\theta(x_{\mathrm{f}}) = 0$. This is a reasonable assumption when the train stops at a station because the track is aligned with the platform, which is usually flat. When the train comes to a standstill at the stopping point, then $\dot{v}(t_{\mathrm{f}}) = 0$ and $v(t_{\mathrm{f}}) = 0$, so that from (5), $\hat{u}(t_{\mathrm{f}}) = 0$. This means that the stopping point is an equilibrium of the system. If the track is not flat at the stopping point, then a finite traction is required to hold the train stationary, although in practice, the external mechanical brake is applied once the train has stopped to avoid this.

Since the gradient is modeled as piecewise constant, the system is piecewise linear, with switches occurring at the points where the gradient changes. Because the aim is to minimise the time required to bring the train to a standstill, this is a minimum time problem [8] and the optimal solution is to apply the maximum braking traction $-\underline{u}$. However, the jerk constraints in (4) limit the braking traction that can be applied at the beginning and end of the braking trajectory, so within each section of the piecewise linear system, one of the constraints will be active and the solution reduces to identifying the points where the system switches between these active constraints.

It is convenient to solve the optimisation problem backwards in time. Define $\tilde{t} = t_{\mathrm{f}} - t$ and denoting differentiation

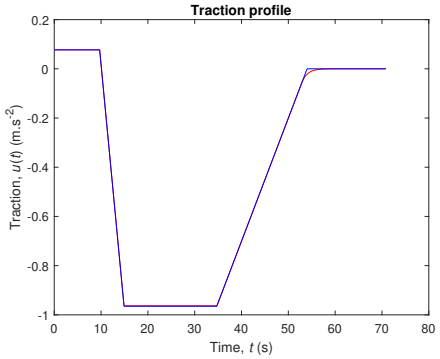

(a) Optimal traction applied to train.

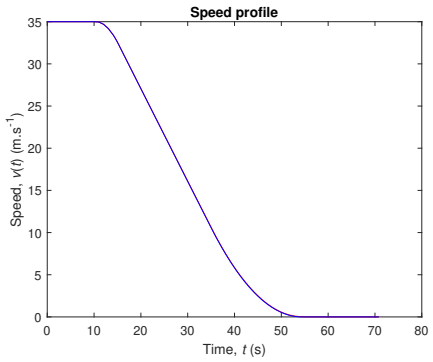

(b) Train speed.

Fig. 1: Solution to minimum time optimisation problem.

with respect to $\tilde{t}$ by $(.)'$, then the optimal state trajectory satisfies

$$\begin{bmatrix} \hat{u}'(\tilde{t}) \\ v'(\tilde{t}) \\ x'(\tilde{t}) \end{bmatrix} = \begin{bmatrix} 0 & 0 & 0 \\ -b^{(i)} & a^{(i)} & 0 \\ 0 & 0 & -1 \end{bmatrix} \begin{bmatrix} \hat{u}(\tilde{t}) \\ v(\tilde{t}) \\ x(\tilde{t}) \end{bmatrix} - \begin{bmatrix} \hat{j}(\tilde{t}) \\ 0 \\ 0 \end{bmatrix} + \begin{bmatrix} 0 \\ g\,\theta(x(\tilde{t}))) \\ 0 \end{bmatrix}. \quad (7)$$

for $\tilde{t} \in [0, t_{\rm f}]$, which is divided into the following segments.

1) Over the time period $\tilde{t} \in [0, \tilde{t}_1]$, the traction is limited by the jerk constraint in (4), so that $\hat{j} = -\bar{j}$ and $\hat{u}(\tilde{t}) = -\bar{j}\tilde{t}$. During this time interval, the traction changes from $\hat{u}(0) = 0$ to $\hat{u}(t_1) = -\underline{u}$, where $\tilde{t}_1 = \underline{u}/\bar{j}$.
2) For $\tilde{t} \in [\tilde{t}_1, \tilde{t}_2]$, the maximum braking traction is applied, so that $\hat{u}(\tilde{t}) = -\underline{u}$.
3) $\tilde{t} \in [\tilde{t}_2, \tilde{t}_3]$, the jerk constraint in (5) is active with $\hat{j} = \underline{j}$, taking the braking traction from $\hat{u}(\tilde{t}_2) = -\underline{u}$ to $\hat{u}(\tilde{t}_3) = -\hat{u}_0$ where $\hat{u}_0$ i given in (6). Since $\hat{u}_0$ depends upon the track gradient, which in turn, is a function of $x(\tilde{t}_3)$, then the trajectory is the solution to a two-point boundary problem, where $\tilde{t}_3$ are unknowns, and $v(\tilde{t}_3) = v_0$, while $v(\tilde{t}_2)$ and $x(\tilde{t}_2)$ are determined from the previous segment of the trajectory.

Because the system is piecewise linear, analytic solutions can

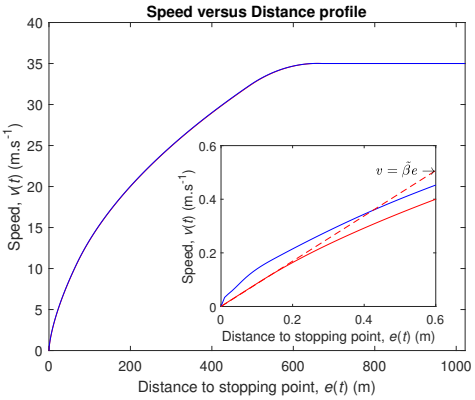

Fig. 2: Speed plotted against distance to stopping point for optimal trajectory (blue) and modified, sub-optimal trajectory (red). Inset shows curves for low speeds when close to stopping point.

be obtained for the first two segment of the trajectory by solving (7) between changes in the track gradient. However, the two-point boundary problem in the third segment of the trajectory needs to be solved numerically. Fig. 1a shows the optimal traction when braking from 126 kph (35 m.s^{-1}) and Fig. 1b shows the corresponding speed during braking. Denoting the distance to the stopping point by $e(t)$, where $e(t) = x_{\rm f} - x(t)$ then Fig. 2 plots the braking curve, $v = \psi(e)$, which relates the speed to the distance to the stopping point. For simplicity, it has been assumed that the track is flat, so that $\theta(x(t)) = 0$ throughout braking.

III. FEEDBACK CONTROL

A. PID Controller

The control system applies the traction profile obtained from the minimum time optimisation problem described in Section II-C as a feedforward input and feedback is used to ensure that the speed follows this desired trajectory. As shown in Figure 3, the reference signal for the inner feedback loop is obtained using the distance of the train from the desired stopping point to determine the desired speed from the braking curve in Fig. 2. The effect of the track gradient on the train is compensated within the feedforward traction signal $u(t)$ and any mismatch between the modeled gradient and the actual gradient is considered as an input disturbance.

From (1), the transfer function during braking between the traction $u(t)$ and the train speed $v(t)$ is

$$P(s) = \frac{b^{\rm B}}{s + a^{\rm B}}\,{\rm e}^{-\tau s}. \quad (8)$$

The speed is regulated by a PID controller that includes a filter on the derivative term with transfer function

$$C(s) = K\left(1 + \frac{1}{T_{\rm I}s} + \frac{T_{\rm D}s}{T_{\rm F}s + 1}\right) \quad (9)$$

where K is the controller gain and $T_{\rm I}$, $T_{\rm D}$ and $T_{\rm F}$ are the time constants of the integral, derivative and filter terms. Using a

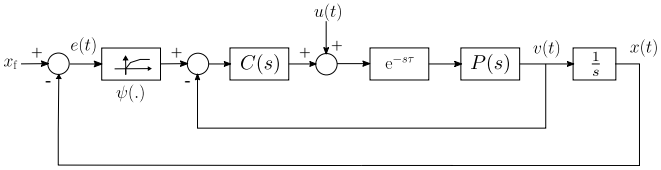

Fig. 3: Block diagram of controlled system.

first order Pade approximation for the delay term in (8), the design of the controller is based on an approximate transfer function

$$P^{\rm a}(s) = \frac{b^{\rm B}}{s + a^{\rm B}} \frac{1 - \tau s/2}{1 + \tau s/2}. \tag{10}$$

Lambda tuning is used to design the PID controller [10], where the transfer function of the controller cancels both the pole at $s = -a^{\rm B}$ associated with the train dynamics and the pole at $s = -2/\tau$ from the Pade approximation of the delay. Following the procedure in [11], for the system parameters in Table I, placing the closed loop poles at $s = -3.5/\tau$, leads to the controller whose terms are given in Table III. For this controller, the gain margin of the inner closed loop is $GM = 10.11$ at $\omega_{\rm G} = 6.29$ rad.s^{-1}, while the phase margin is $PM = 83.53^\circ$ at $\omega_{\rm P} = 0.50$ rad.s^{-1}, indicating that the controller is robust to uncertainties in both the system dynamics and the time delay. Although lambda tuning provides good tracking of the desired speed obtained from the braking curve, because the train dynamics are lag dominated, there is a risk that the pole-zero cancellation can make the controller slow to respond to traction disturbances [10], although from simulations, this was not found to be an issue.

K (s^{-1})	$T_{\rm I}$ (s)	$T_{\rm D}$ (s)	$T_{\rm F}$ (s)
0.44	3.8×10^3	0.075	0.075

TABLE III: Values of controller parameters.

Remark 1. In practice, positive traction cannot be applied during the braking phase, so the traction is limited to $u(t) \leq 0$. As a result, it is necessary to include anti-windup in the PID controller to avoid integral windup [10].

Remark 2. Although the feedforward traction profile is designed to accommodate the constraint on the maximum braking traction in (3), the actual limit on the magnitude of the braking traction needs to be higher than $\bar{u}$ to allow for corrections to the traction from the PID controller to be applied. In this study, $\bar{u}$ is set to 80% of the hard limit.

B. Outer Feedback Loop

As shown in Fig. 3, the speed set point for the inner feedback loop is determined from the braking curve $v = \psi(e)$ in Fig. 2. Because the train cannot reverse during the braking phase, when the train goes past the stopping point, which means that the distance to the stopping point is negative, the speed set point is zero, so that $\psi(e) = 0$ for $e \leq 0$. The braking curve, $\psi(.)$, is a memoryless, static nonlinearity [9], which is sector bounded with $\psi(.)$ belonging to the sector $[0, \infty]$, so that the outer feedback loop can be considered as a Lur'e system [9]. The stability of the closed loop system can be determined using the Popov criterion [9]. Define

$$G(s) = \frac{1}{s} \frac{P^{\rm a}(s)C(s)}{1 + P^{\rm a}(s)C(s)} \tag{11}$$

and using a Lyapunov function of the form $V = (1/2)q^{\rm T}Pq + \lambda \int_0^q \psi(\sigma){\rm d}\sigma$, where q is a state of $G(s)$, $P = P^{\rm T}$ is a positive definite matrix and $\lambda > 0$, then the closed loop system will be absolutely stable if $(1 + s\lambda)G(s)$ is positive real [9]. If $G(s) \sim \left[\begin{array}{c|c} A & B \\ \hline C & 0 \end{array}\right]$ is a minimal realisation of $G(s)$, then the system is absolutely stable [9] if there exists P, λ and $M > 0$, such that [9], [12]

$$\left[\begin{array}{cc} A^{\rm T}P + PA & PB - C^{\rm T} - A^{\rm T}C^{\rm T}\lambda \\ B^{\rm T}P - \lambda CA - C & -2M - \lambda CB - B^{\rm T}C^{\rm T}\lambda \end{array}\right] < 0 \tag{12}$$

provided that the braking curve belongs to the sector $\psi \in [0, \beta]$, where $\beta = 1/M$. For the values of the system parameters in Table I and the controller parameters in Table III, $\beta = 4.32$ and $\lambda = 1.80$.

C. Modified Feedforward Traction

The criterion for stability based on the Popov criterion shows that the closed loop system will be stable if the static, memoryless nonlinearity associated with speed distance profile in Fig. 2 belongs to the sector $[0, \beta]$. However, because ${\rm d}v/{\rm d}e \to \infty$ as $e \to 0$, the profile belongs to the sector $[0, \infty]$, the criterion for stability cannot be guaranteed. To satisfy the criterion, the optimal feedforward policy can be modified by identifying the point e_β at which

$${\rm d}v/{\rm d}e|_{e=e_\beta} = \beta \tag{13}$$

and then changing the optimal traction to ensure that the slope of the speed distance profile is constant for all values of x below this value. Because this is the limiting value of β to ensure stability, in practice, the limiting value of the slope is set to $0 < \tilde{\beta} < \beta$ and for this study, a value of $\tilde{\beta} = 0.1\beta$. Since $e(t) = x_{\rm f} - x(t)$, then the condition can be expressed as ${\rm d}v/{\rm d}x = -\tilde{\beta}$, which will be satisfied when $v(t) = A{\rm e}^{-\tilde{\beta}t}$, where $A > 0$ is a constant, so that $x(t) = -(A/\tilde{\beta}){\rm e}^{-\tilde{\beta}t}$. Note that when $x_{\rm f}$ is taken as zero, then $x(t) \leq 0$. Using (5), the feedforward traction $\hat{u}(t)$ can be obtained. This has the effect of adding an "exponential tail" to the optimal solution, which modifies the feedforward trajectory as the train comes to a standstill, as shown by the red curves in Figs. 1 and 2. The effect of the modification is most clearly seen in the inset in Fig. 2, which shows that the slope of the modified braking curve is limited to $\tilde{\beta}$ as the speed approaches zero. The constant A is chosen to match $\hat{u}(t)$ the jerk limit $\bar{j}$ to ensure a jerk free transition between the optimal trajectory and the exponential tail. Because the speed follows an exponential decay, then technically the train will not come to a standstill, but in practice, when the magnitudes of the traction and the speed are small, an external mechanical brake is applied, bringing the train to a halt.

IV. RESULTS

A. Simulated Model

The response of the system is simulated using Simulink for $P(s)$ described by (2) with the parameters in Tab. I and the PID controller $C(s)$ in (9) with the parameters in Tab. III. The blue line in Fig. 4a shows the optimal, minimum time feedforward traction when braking from 35 m.s^{-1} (126 kph) at 10 s. The red line in the plot shows the applied traction and the difference between the two signals is the correction applied by the PID controller. Fig. 4b shows the reference speed (blue) and the actual speed (red) and although the actual speed closely follows the reference speed, there is some error, as shown by the inset in Fig. 4b. During the period from about 15 s to 35 s, when the traction is constant, the reference speed has a constant slope, which can be followed by the actual speed due to the integrator in outer feedback loop. However, as the train approaches the stopping point, the slope of the braking curve that determines the reference speed becomes unbounded, leading to oscillations in the applied traction, which results in an increase in the speed error as the train comes to a standstill.

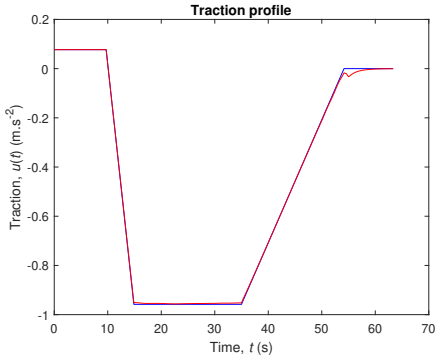

(a) Optimal traction profile (blue) and actual traction applied to train (red).

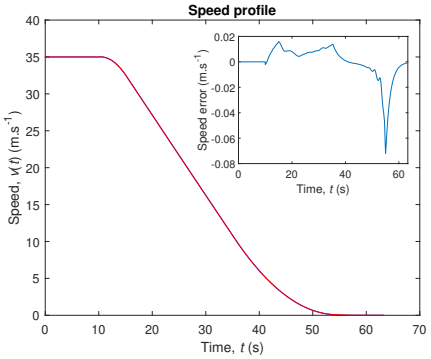

(b) Reference train speed (blue) and actual train speed (red). Inset shows error in speed.

Fig. 4: Simulated response for minimum time optimal response without reduced gain at low speeds.

Fig. 5 shows the corresponding plots associated with the sub-optimal feedforward trajectory that limits the slope of the braking curve at low speeds. From Fig. 5a, the “exponential" decrease in the feedforward braking traction as the train comes to a standstill can be seen and unlike the optimal trajectory in Fig. 4a, the applied traction closely follows the feedforward signal without oscillations, leading to smoother braking without large jerks. The magnitude of error in the speed in the inset in Fig. 4b is also smaller. Although the “exponential" section increases the length of the sub-optimal trajectory by about 5 s, this is offset in the actual response as the sub-optimal trajectory does not need to settle following the oscillations in the actual traction observed in Fig. 4a, so in practice, the braking time for the sub-optimal trajectory is not increased.

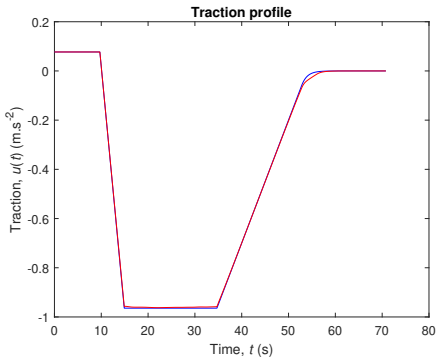

(a) Optimal traction profile (blue) and actual traction applied to train (red).

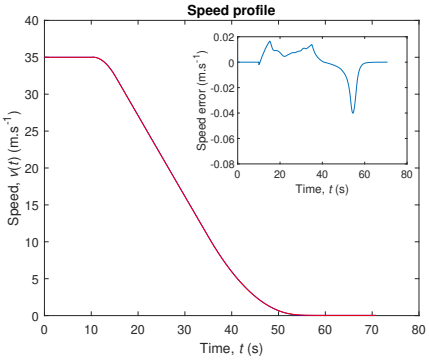

(b) Reference train speed (blue) and actual train speed (red). Inset shows error in speed.

Fig. 5: Simulated response for sub-optimal response with reduced gain at low speeds.

B. Simulation of Industrial Model

Although the simplified model of the train dynamics in (1) captures the dominant behavior of the system, the actual response is more complicated. To evaluate whether the combination of a feedforward strategy and the PID controller that is based on a simplified model is sufficiently robust to be applied to a real train, the system was evaluated on a simulation that used a more accurate model of the train dynamics provided by Siemens Mobility GmbH. This simulation includes the change in the dynamics associated with

the switches between regenerative and pneumatic braking, as well as the effects of the discrete measurements of the train position taken by the individual sensors along the track and the deadzone that limits the magnitude of the smallest traction that can be applied to the train. Fig. 6 shows the results of the simulation when using the PID controller with the sub-optimal feedforward trajectory in Fig. 5 when braking from 35 m.s^{-1}. From the traction profile in Fig. 6a, it can be seen that the response of the full model is more complicated than the response of the simplified model and changes in the dynamics associated with different modes of braking can be observed around 40 s and 50 s. The effect of the quantisation due to the discrete sampling introduces a sawtooth signal on the traction signal. Despite this, the PID controller is able to ensure that the applied traction follows the feedforward traction curve, so that the magnitude of the error in the speed does not exceed 0.4 m.s^{-1}. Although the braking takes place over a distance of 639 m, the stopping error is only 13 cm.

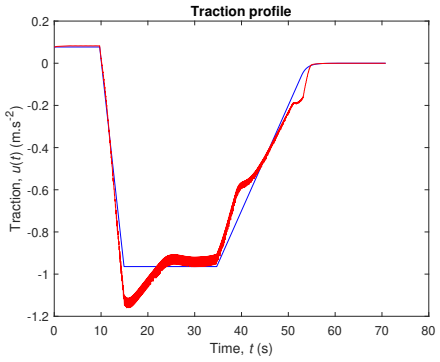

(a) Optimal traction profile (blue) and actual traction applied to train (red).

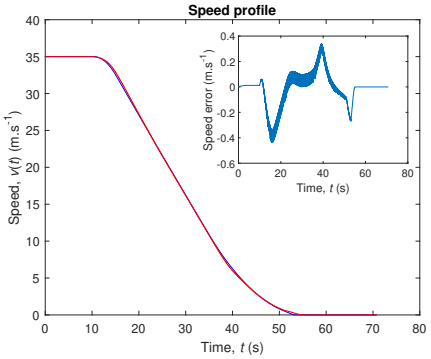

(b) Reference train speed (blue) and actual train speed (red). Inset shows error in speed.

Fig. 6: Response of industry supplied model for sub-optimal response with reduced gain at low speeds.

V. CONCLUSIONS

This paper has presented a method of braking a train so that it stops at a specific location in minimum time. The system forms a component of an ATO system. The approach is based on applying braking traction obtained by solving a minimum time optimisation problem as a feedforward signal and then using feedback to ensure that the train speed follows the desired braking curve, which relates the speed to the distance from the stopping point. To reduce the computational load and to align with the existing system, the feedback uses a PID controller, which is designed to be robust to uncertainties in the train dynamics. The braking curve is a sector bounded, static nonlinearity, so the controller can be considered as a Lur'e system, and using the Popov criterion, the limit on the slope of the braking curve can be found that ensures that the system is absolutely stable. The optimal solution is modified to satisfy this condition and simulations demonstrate that this avoids oscillations in the braking traction as the train approaches the stopping point. Current research is evaluating the performance of the controller for a range of trains over different operating conditions.

VI. ACKNOWLEDGMENTS

The authors are grateful to Siemens Mobility GmbH for providing the industrial model used in the simulation in Sect. IV-B.

REFERENCES

[1] S. Aradi, T. Bécsi, and P. Gáspár, "Design of predictive optimization method for energy-efficient operation of trains," in *2014 European Control Conference (ECC)*, 2014, pp. 2490–2495.

[2] W. Zhong, S. Li, H. Xu, and W. Zhang, "On-line train speed profile generation of high-speed railway with energy-saving: A model predictive control method," *IEEE Transactions on Intelligent Transportation Systems*, vol. 23, no. 5, pp. 4063–4074, 2022.

[3] H. Farooqi, L. Fagiano, P. Colaneri, and D. Barlini, "Efficient train operation via shrinking horizon parametrized predictive control," *IFAC-PapersOnLine*, vol. 51, no. 20, pp. 203–208, 2018.

[4] ——, "Shrinking horizon parametrized predictive control with application to energy-efficient train operation," *Automatica*, vol. 112, p. 108635, 2020.

[5] H. Homburger, S. Wirtensohn, M. Diehl, and J. Reuter, "Energy-optimal planning and shrinking horizon MPC for vessel docking in river current fields," in *2024 European Control Conference (ECC)*, 2024, pp. 1125–1130.

[6] S. Wirtensohn, O. Hamburger, H. Homburger, L. M. Kinjo, and J. Reuter, "Comparison of advanced control strategies for automated docking," *IFAC-PapersOnLine*, vol. 54, no. 16, pp. 295–300, 2021.

[7] W. B. Greer and C. Sultan, "Shrinking horizon model predictive control method for helicopter–ship touchdown," *Journal of Guidance, Control, and Dynamics*, vol. 43, no. 5, pp. 884–900, 2020.

[8] A. E. Bryson and Y. Ho, *Applied Optimal Control*. New York, NY: Routledge, 1975.

[9] H. K. Khalil, *Nonlinear System*, 3rd ed. Upper Saddle River, NJ: Prentive Hall, 2002.

[10] K. J. Åstrom and T. Hägglund, *Advanced PID Control*. Research Triangle Park, NC: International Society of Automation, 2006.

[11] A. J. Isaksson and S. F. Graebe, "Derivative filter is an integral part of PID design," *IEE Proceedings Control Theory and Applications*, vol. 149, no. 1, pp. 41–45, 2002.

[12] S. Boyd, L. El Ghaoui, E. Feron, and V. Balakrishnan, *Linear Matrix Inequalities in System and Control Theory*. Philadelphia, PA: SIAM Studies in Applied Mathematics, 1994.